JOURNAL OF MATERIALS SCIENCE 24 (1989) 3311–3318

Deformation of oriented high density polyethylene shish-kebab films

Part 1 *Decrystallization at room temperature*

JEAN M. BRADY*, EDWIN L. THOMAS
Department of Polymer Science and Engineering, University of Massachusetts, Amherst, Massachusetts 01003, USA

Decrystallization is defined as the mechanically induced reduction and reorganization of the crystalline phase. The decrystallization of oriented high density polyethylene (HDPE) was observed here by transmission electron microscopy (TEM). A special drawing technique was used to form thin films with an idealized, highly oriented, shish-kebab morphology. These oriented films were uniaxially elongated at room temperature along or perpendicular to the chain direction, and then viewed by TEM. The use of such a well defined initial morphology reduced the deformation of polyethylene as a whole to that of three structural elements: long shish crystals, chain folded kebabs, and the non-crystalline phase. The non-uniform deformation characteristic of spherulitic film, in which the elongation direction is parallel to lamellar normals in one region and perpendicular to them in another, was thus avoided. High strain transformed the shish-kebab morphology into filaments which were generally non-crystalline and of uniform diameter, with occasional crystalline remnants within them. Upon decrystallization, internal "defects" were generated within crystallites, facilitating subsequent yielding. Stressed kebabs decrystallized and fed into the shish core. "Defect" generation also resulted in a reduction in crystal thickness along the chain direction, indicating that such a reduction can occur in the absence of thermally induced melting. Crystals underwent $\langle 0\,0\,1 \rangle$ crystal shear and chain slip, reducing crystal width, as well as martensitic transformation to the monoclinic crystalline form. No subsequent recrystallization was detected by darkfield studies. The influence of the initial shish-kebab morphology of undeformed films on the growth of crazelike structures was discussed.

1. Introduction

Much research has been devoted to understanding the dependence of the mechanical properties of semicrystalline polymers on morphology and molecular topology [1–8]. In particular, emphasis has been placed on developing structural models which relate morphology to deformation behaviour and overall mechanical properties. The present article is concerned with the deformation behaviour of polyethylene (PE). The structure–mechanical property models of PE can be divided into two main categories. One type is applicable to very highly crystalline, highly oriented ultradrawn material in which the structure is approximated by a crystalline continuum containing various defects. The other type is applicable to low draw ratio semicrystalline polymers, which can be viewed as oriented two-phase composite materials [9–11]. The application of two-phase composite models to describe semi-crystalline polymers is not as straightforward as it may seem. Difficulties are often encountered when defining the two phases with respect to specific load-bearing morphological elements [11]. Indeed, the parallel–series arrangements of phases in mechanical models are often primitive representations of the actual morphology of the sample. Nonetheless, such arrangements can be used to describe morphological extremes. Two-phase models are relevant to the present studies, and will be discussed in more detail below.

One of the most well known two-phase deformation models was introduced in 1971 by Peterlin for semicrystalline polymers [3, 12]. In his model, stressed spherulitic lamellae shear into crystal blocks via chain tilt within lamellae and longitudinal slip at mosaic block interfaces. The blocks rotate such that the molecular axes align along the local principal stress direction. For PE, this deformation is often accompanied by crystal twinning and the conversion from orthorhombic to monoclinic crystals [13, 14]. The crystal blocks decrease in width by chain slip and unfolding until a microfibril of alternating crystal–amorphous regions is formed. Each lamellar stack forms numerous micronecks once the yield stress is reached. Each microneck in turn, is associated with the formation of a microfibril, the basic structural element of this model.

Present address: Mobil Chemical Company, Research and Development, PO Box 240, Edison, New Jersey 08818-0240, USA.

0022–2461/89 $03.00 + .12

In Peterlin's model, microfibrils which have experienced approximately the same local strain history coalesce to form a fibril in which the registry between microfibrils is quite good. Interfibrillar tie molecules connect both adjacent fibrils as well as microfibrils, and in addition to Van der Waals forces comprise the "frictional" forces which resist longitudinal slip between fibrillar elements. Intermicrofibrillar tie molecules are believed to arise not only from the tie molecules which interconnect lamellae in the original structure, but also are formed by the unfolding and elongation of chains during microfibrillar slip. This results in a large number of tie molecules being located on the outer surface of microfibrils [15]. It is generally believed that upon straining, tie molecules become taut by undergoing gauche to trans conformational changes [3]. Further straining results in bond angle distortion and the stretching of covalent bonds. Ultimately, some taut tie molecules undergo chain scission while other ones take on the additional load as strain increases. According to Peterlin, the increase in tensile modulus with strain can, at least in part, be explained in terms of an increase in the number of taut tie molecules. Controversy over the location of such taut tie molecules within the context of a microfibrillar model has led to variations of the original Peterlin model [16, 17].

In the revised Peterlin model [3, 18], reinforcing elements consist not only of interfibrillar tie molecules, but also of crystalline bridges and taut intrafibrillar tie molecules which span the amorphous layers between lamellae within a microfibril. The incorporation of crystalline bridges has proven particularly useful in explaining the time dependence of mechanical properties in PE. For instance, the tensile modulus of PE decreases during annealing, and subsequently recovers upon cooling and ageing at room temperature [18, 19]. It is believed that the crystalline bridges melt during annealing, and subsequently recrystallize upon cooling. The formation of crystalline bridges is further substantiated by the fact that the tensile modulus of as-drawn PE increases and the permeability decreases as the material is aged at room temperature [20]. Previous studies have in fact shown that polyethylene undergoes chain reorganization and crystallization at room temperature [21].

Some small angle X-ray scattering measurements have indicated that the average crystal thickness and long period in the deformed material differ from those in the undeformed material and depend only on the drawing temperature [22–24]. This was originally interpreted to mean that the conversion of lamellae to microfibrils involved a rise in temperature and subsequent melting and recrystallization during drawing [23]. Subsequent temperature rise calculations suggested, however, that the temperature rise associated with necking would be insufficient to melt lamellae [24]. Instead, the reorganization of the crystalline phase was believed to be primarily mechanically induced although little published direct evidence exists.

This paper is Part I of a two-part series devoted to detailing and understanding the mechanisms by which polyethylene reorganizes under stress. Thin shish-kebab morphology HDPE films were slowly uniaxially elongated at room temperature. In light of the low elongation rate employed and the thinness of films, it is believed that drawing was near isothermal. Such drawing conditions would result in a slow rate of energy release, and a relatively fast rate of heat dissipation, respectively. Thus the present studies will involve direct visualization of morphological transformations which occur without a significant accompanying rise in temperature. Part II [25] of this series is concerned with deformation at elevated temperatures, the overall goal concentrating on the evolution of crystalline phase continuity with drawing. Evidence suggesting the formation of a sample-spanning crystalline phase in ultradrawn polyethylene and the mechanisms by which it forms will be addressed [25, 26].

2. Experimental details

2.1. Materials and processing

The polymer used was Marlex 6003, obtained from Phillips Petroleum Corporation, with $M_w = 200\,000$ and $M_w/M_N = 7$ to 13. Thin films were prepared using the technique of Petermann and Gohil [27]. A full description of the film preparation techniques used in this study, as well as the morphological characterization of as-drawn films can be found in a previous publication [28]. The rotation angle between images and diffraction patterns was calibrated by comparing the orientation of the image and shape transform of a MgO single crystal (vapour deposited onto a carbon film).

2.2. Microscopy

For deformation studies, thin (100 nm × 2 mm × 4 mm) films were placed on annealed (typically 700° C for 18 h *in vacuo*) electroformed copper deformation grids which were purchased from Interconics of St Paul, Minnesota. To promote film adhesion to grids, the grids were pretreated by immersing them in hot polyethylene solution and subsequently drying them. Samples were then floated onto the grid from a water surface. The grid and supported film were uniaxially elongated at a nominal rate of 5×10^{-4} mm sec^{-1} at room temperature using a JEOL SEH deformation stage. Although films were subjected to an elongational force along the chain direction, a biaxial planar stress field developed due to hindered lateral contraction of the film. Typically, a 0.5 to 1.0 mm gauge length sample was elongated by 0.6 mm. The local strain within these films was usually very inhomogeneous and could not be related to the nominal strain.

Films were viewed in brightfield and darkfield modes using a JEOL 100 CX TEM, operated at 100 kV. To avoid the introduction of artifacts and to get the best resolution, no heavy metal stains, gold decoration, replication techniques, or substrate films were used. Low electron dosage precautions were taken to mitigate the electron beam damage incurred by the sample. As can be seen in Fig. 1, the crystalline phase of polyethylene is highly susceptible to beam damage.

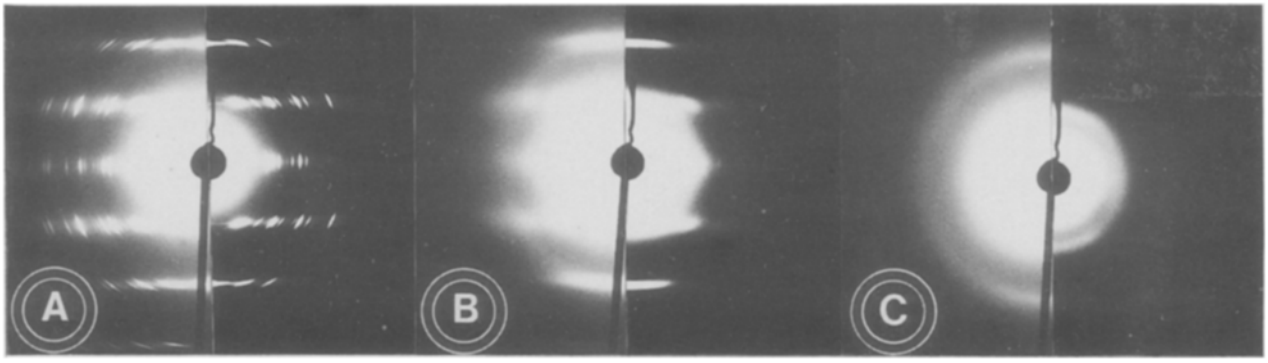

Figure 1 Electron diffraction patterns illustrating the effect of electron irradiation on order in polyethylene crystals. The radiation dose increases from a to c. Each diffraction pattern is shown at two different exposures. Chain axis vertical here and in subsequent figures unless stated otherwise.

3. Results and discussion

3.1. Morphology of undeformed film

The morphology of undeformed film was an idealized one comprised well oriented lamellar stacks (Fig. 2). The lamellae were in turn made up of mosiac blocks which were approximately as wide (27 nm, perpendicular to the chain axis) as they were thick (parallel to the chain axis). Electron diffraction indicated a high degree of chain axis orientation as well as a single crystal like texture in which the *a* axis was preferentially oriented perpendicular to the film plane and the *c* axis was oriented along the draw direction. The shish nature of these films was generally not readily apparent until they were deformed. The fact that such an idealized initial morphology was used greatly simplified these deformation studies, since the film could be elongated along a well defined direction with respect to lamellar normals. Moreover, since both shish and kebab elements were clearly distinct, the response of shish-kebabs to elongational forces could be studied in great detail.

3.2. Elongation parallel to the chain direction

At low strains, the polyethylene films deformed elastically by elongation of the non-crystalline phase [21]. The details of deformation at low strains were not observed here. However, such elongation would occur freely only in regions not reinforced by shish crystals, and would, therefore, not occur uniformly throughout the sample. Longitudinal forces (parallel to the chain direction) would elongate material at the ends of shish-kebabs while lateral forces (perpendicular to the chain direction) would elongate material between shish crystals. When films were highly strained along the chain direction, an increase in the longitudinal separation between lamellae was seen (Fig. 3a), resulting in the formation of craze-like cavities within the intervening non-crystalline regions. Crazes have been seen previously in PE, and involve deformation not only of the amorphous phase but the crystalline phase as well [29, 30]. The numerous short cavities seen here, which resulted from amorphous phase extension along the chain direction, did not propagate laterally. Growth was apparently arrested by shish crystal reinforcement.

The non-crystalline phase was subject to fewer constraints to extension in the lateral direction than parallel to the chain direction. Longitudinal and lateral stresses which developed were relieved by film thinning, and cavitation (Fig. 3a). Eventually, these cavities coalesced, resulting in the growth of elongated voids between shish-kebabs (Fig. 3b), and the formation of craze-like structures which propagated parallel to the chain direction (Fig. 3c). Cavity-spanning fibrils were believed to consist of tie molecules and entangled chains as well as free chain ends. It is clear that lateral film strength ultimately depends on the number density and strength of the load-bearing fibrils. The interconnected nature of the various structural elements in these films resulted in a network-like appearance similar to that found elsewhere [31] (Fig. 3d). This is

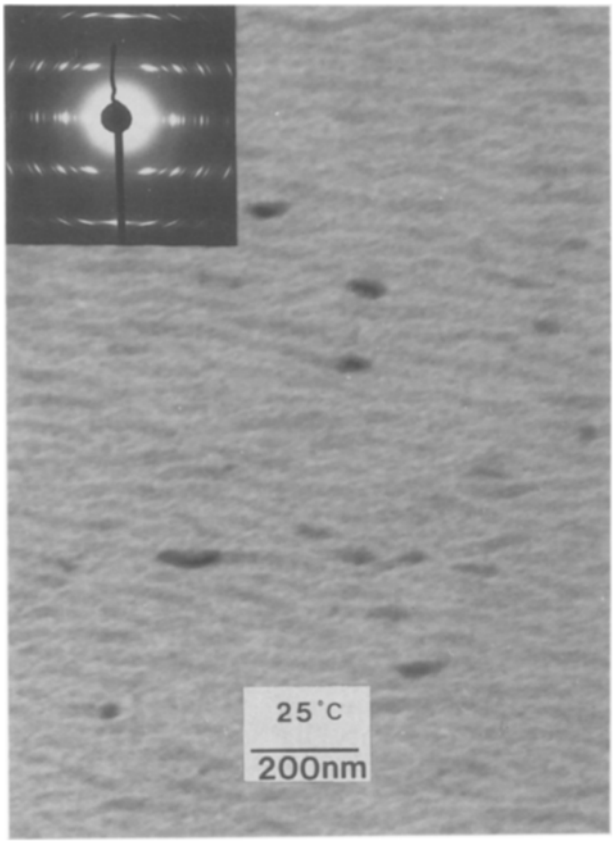

Figure 2 Undeformed HDPE film with corresponding electron diffraction pattern showing lamellar morphology.

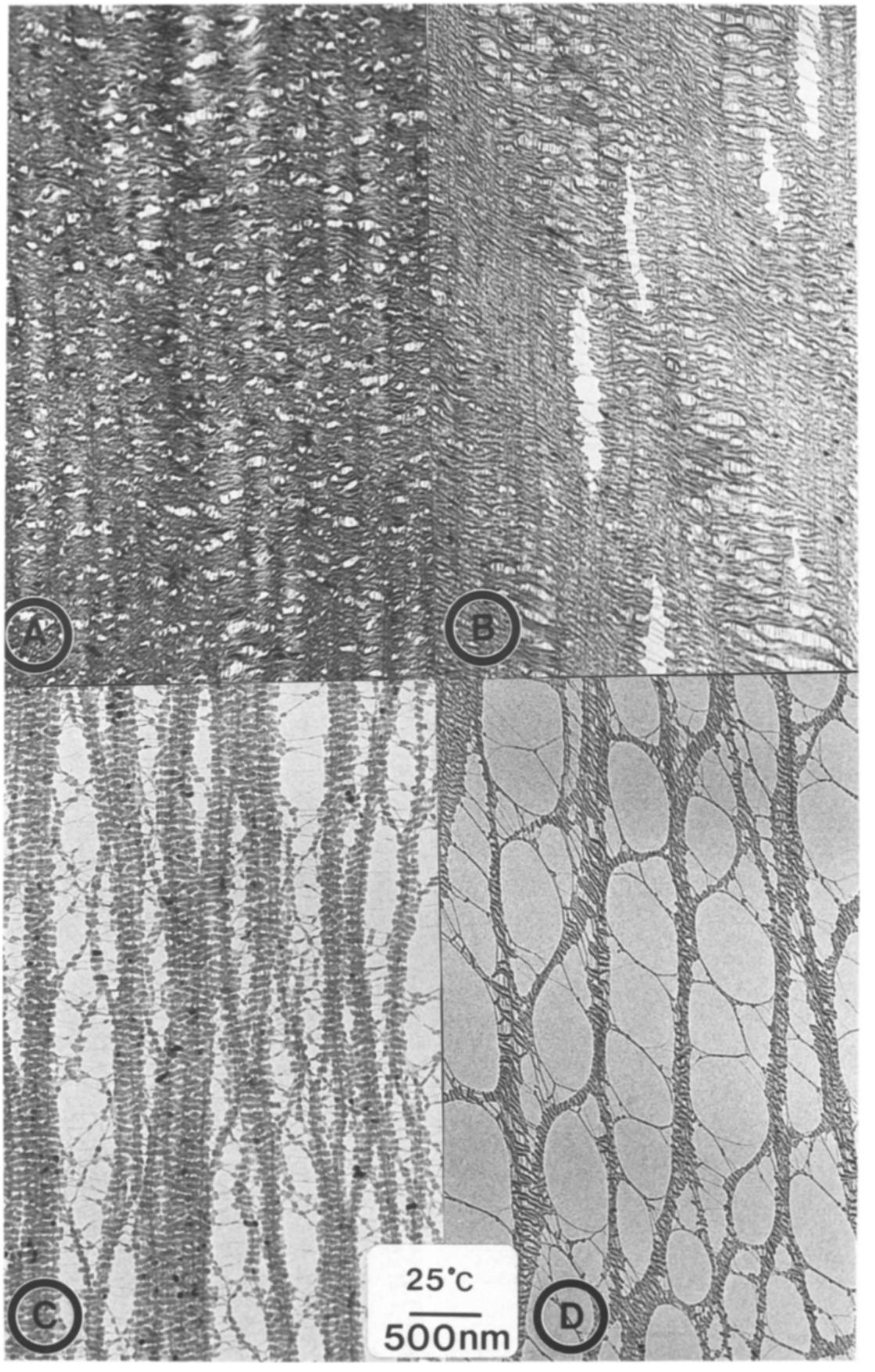

Figure 3 The stages of deformation for HDPE uniaxially elongated along the chain direction: (a) cavitation between lamellae, (b) longitudinal coalescence of cavities into voids, (c) further void formation with individual shish-kebabs now evident, and (d) "network" formation.

consistent with the formation of a gel during the crystallization of PE [28, 32].

Deformation processes in which cavitation preferentially occurred in non-crystalline areas and shish-kebabs peeled apart at the kebab–kebab interface, are summarized in Fig. 3. Details of the later stages of cavitation and fibrillation are best seen at higher magnification (Fig. 4). Shish crystals were clearly visible as dark striations running along the elongation direction. Cavity-spanning fibrils almost

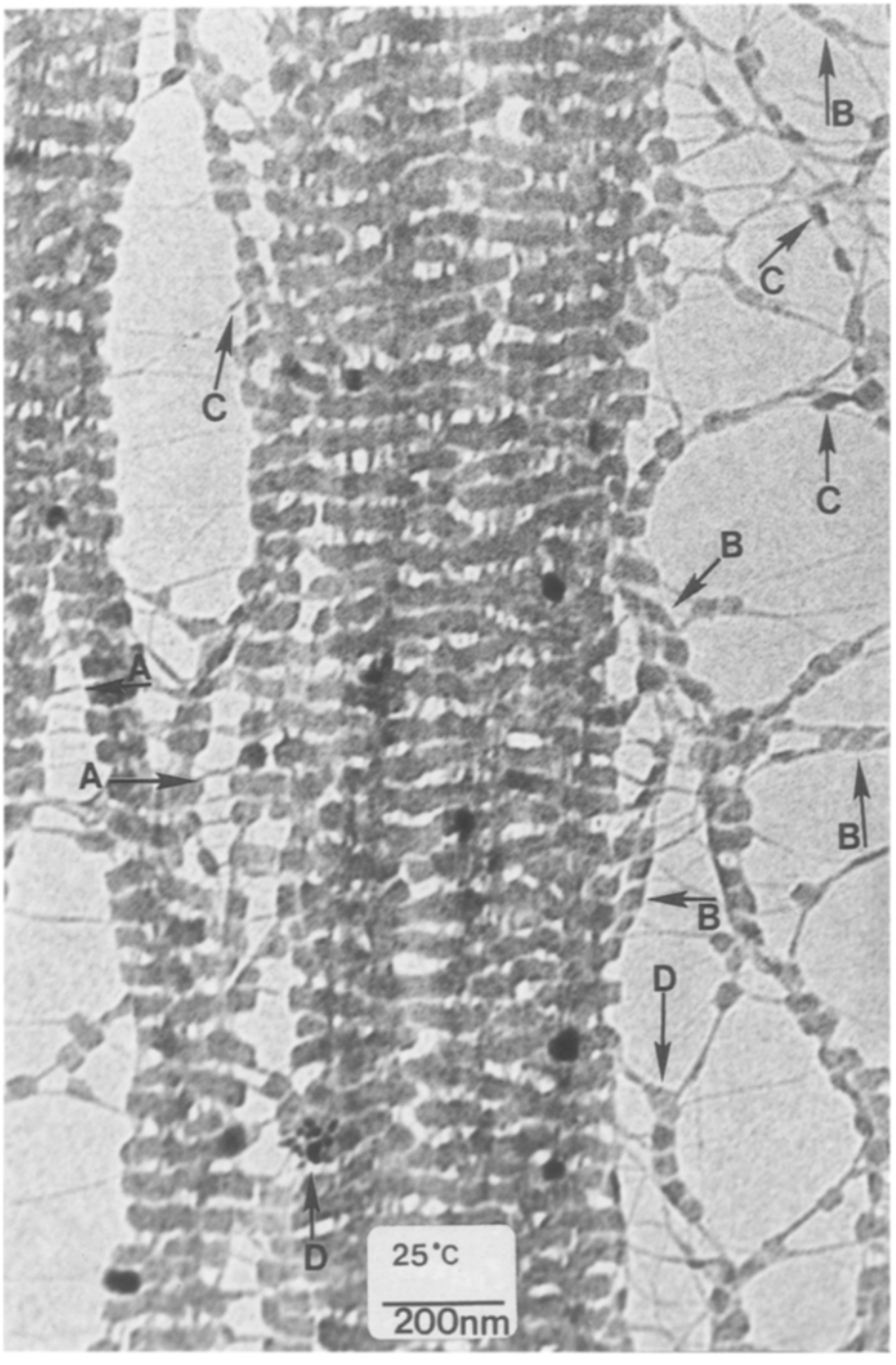

Figure 4 Higher magnification brightfield micrograph of a portion of Fig. 3c. Tie fibrils (A), change in mosaic block shape at early stages of crystal shear (B), crystal shear (C), resulting in a reduction in crystal width, and defective regions within crystals (D).

exclusively originated and terminated at kebab fold surfaces (Fig. 4, region A). At the early stages of deformation, the highly crystalline shish-kebabs remained largely unaltered while the non-crystalline phase underwent extension and cavitation. The stresses transferred by fibrils eventually became sufficiently large to induce the mechanical transformation (decrystallization) of the crystals to which they were attached (Fig. 4, regions B–D). The transformation of shish-kebabs was accompanied by a transition to the monoclinic crystalline phase, as evidenced by the appearance of a (0 0 1), 0.455 nm monoclinic reflection [33]. Chain scission is likely to have occurred as well.

In accord with previously cited microfibrillar mechanical models, crystal blocks in the stressed film pulled apart and fed into fibrils (shish crystals in this case). Thus the crystalline phase was reorganized by mechanical means. Decrystallization occurred via chain slip, crystal shear, and "defect" generation (Fig. 5). Previous studies have indicated that deformation is accompanied by (1 0 0) ⟨0 0 1⟩ and (0 1 0) ⟨0 0 1⟩ crystal shear [34] as well as the generation of new grain boundaries, presumably by a dislocation mechanism [35, 36]. The onset of such shear within mosaic blocks was clearly identified here by changes in block shape from orthorhombic to that of a parallelopiped (Fig. 4, regions B). Subsequent shear resulted in a decrease in crystal width (perpendicular to the chain direction) (Fig. 4, regions C).The generation of "defects" within the interiors of mosaic blocks was detected by the appearance of very localized non-diffracting regions within diffracting mosaic blocks (Fig. 4, regions D). Apparently, these non-diffracting regions had become sufficiently aperiodic to preclude diffraction. The development of such regions provided a mechanism

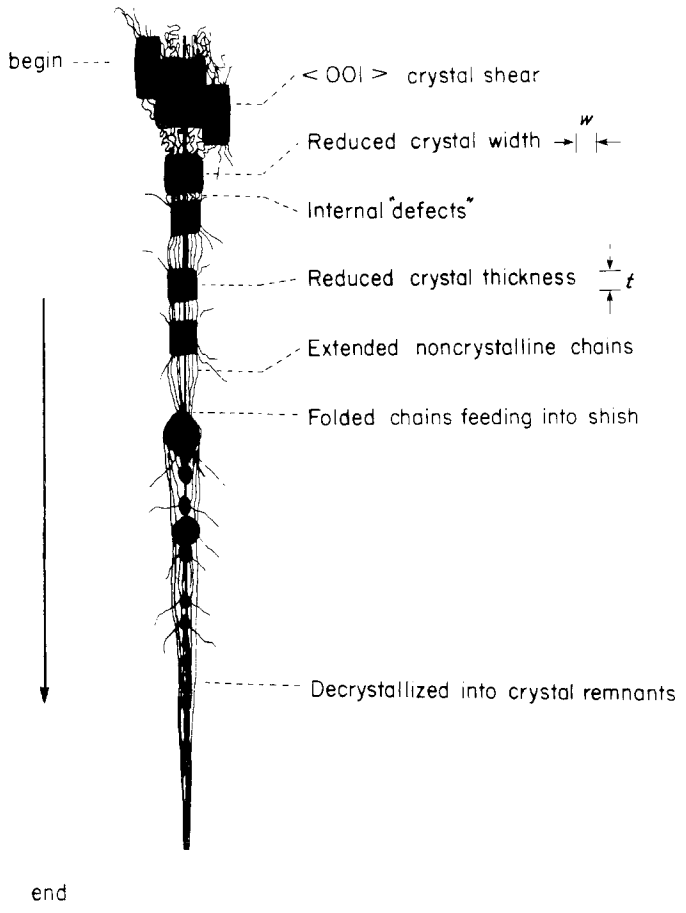

Figure 5 Schematic of decrystallization starting with chain-folded lamellae and ending with decrystallized lamellar remnants.

by which mosaic blocks could reduce their thickness upon deformation, even under near isothermal deformation conditions. Reductions in crystal size could conceivably lead to the thermodynamic destabilization of crystallites, reducing their melting "point" to the extent that melting would occur at the deformation temperature, without invoking a rise in temperature. Indeed, the term "decrystallization" was used here to avoid association with thermally induced melting.

The deformation of bulk polymers has often been associated with a temperature rise sufficiently large to bring about thermally induced melting [22, 23, 37, 38], as well as to facilitate crystal shear by thermal expansion of the crystalline lattice [24, 39]. Changes in crystalline phase morphology with drawing are routinely associated with such melting and recrystallization phenomena. In contrast, the present set of experiments indicate that the yielding processes encompassed by decrystallization can also give rise to extensive morphological change. Most importantly, significant structural evolution is not exclusively a product of melting and recrystallization.

Previous scanning electron microscopy studies of the deformation of solution grown shish-kebabs indicated that kebab size was reduced and the spacing between kebabs increased with draw [40, 41]. In the present case, the deformation process was seen at high resolution without the aid of contrast enhancement techniques such as metal deposition. Indeed, the feeding of kebabs into shish crystals during drawing was clearly indicated by the presence of (about 10 nm thick) crystal remnants throughout fibrils. Moreover, the polydispersity in fibril diameter suggested that draw-down (creep) also occurred. Analogies can be drawn between the way in which kebabs fed into shish crystals during elongation, and the surface drawing mechanism of fibril growth seen in polystyrene crazes [42].

3.3. Elongation perpendicular to the chain direction

Additional experiments were performed to determine the effect of elongating perpendicular to the chain direction. At low strains, cavities grew between shish-kebabs. This enabled the shish-kebabs to rotate by 90 degrees, forming a craze-like structure in which shish-kebabs served as craze fibrils and the chain axis became aligned with the draw direction (Fig. 6). The small arrows in Fig. 6 indicate the direction of lamellar normals on either side of the cavity interface. The rotation of shish-kebabs during deformation was indicative of a high stress level along fibrils. Apparently, "crazing" was facilitated due to the fact that the cavities could propagate between shish-kebabs in the relatively ductile non-crystalline phase. Within the craze-like structure, deformation was essentially identical to that of films deformed along the chain direction. Crystal blocks appeared relatively undeformed until the neck interface was reached. The experimental microstructure shown in Fig. 6 displays all of the schematic components proposed by the Friedrich model [29] except in the present case cavity-spanning

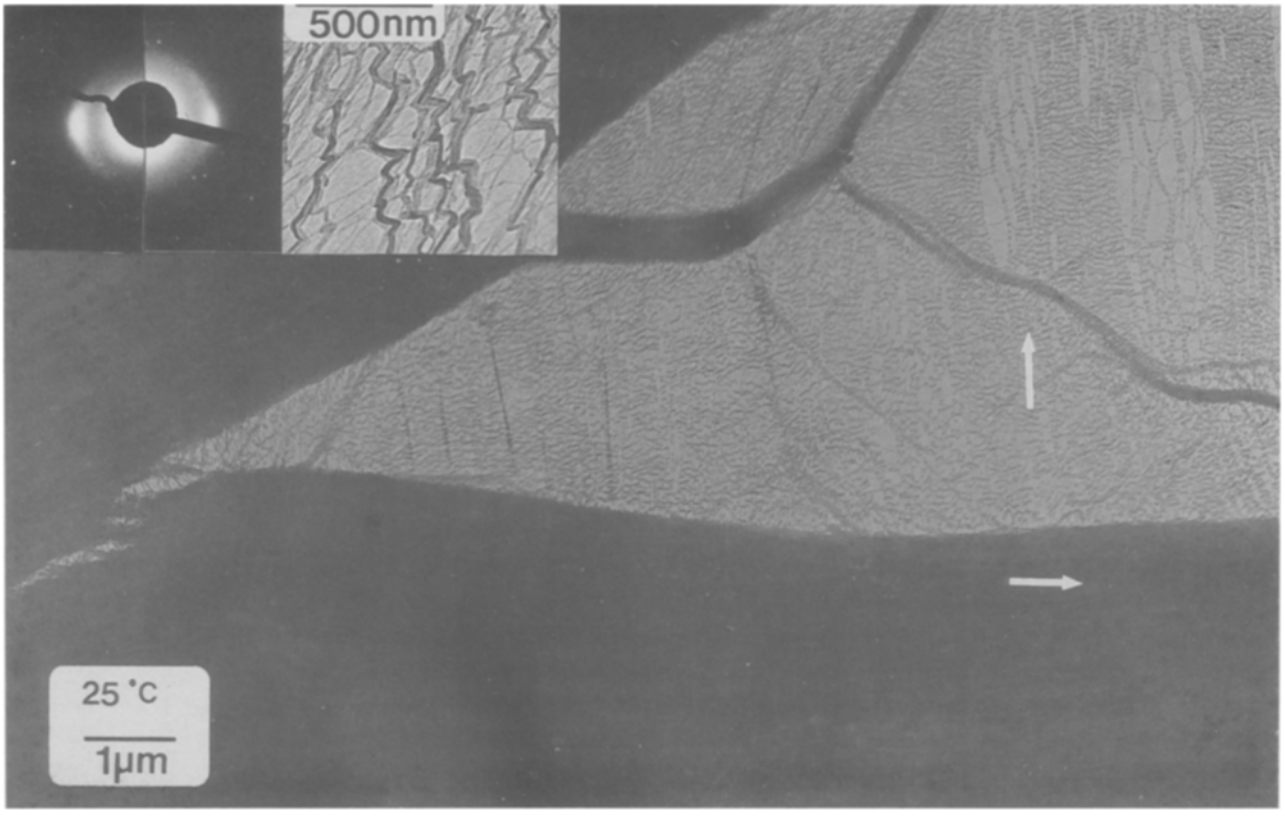

Figure 6 Brightfield micrograph of HDPE film elongated perpendicular to the chain axis showing the formation of craze-like structures as well as 90° rotation of shish-kebabs at cavity interface. Arrows indicate direction of lamellar normals. Insets show the electron diffraction pattern of fibrils within "crazed" regions, as well as the "zigzag" appearance of shish-kebabs under tension within a cavity. Elongation direction vertical.

fibrils were laterally interconnected by tie fibrils. Such connections are clearly seen in Fig. 6. In fact, the lateral separation of cavity-spanning fibrils, and the high tension in tie fibrils often imparted a "zig-zag" appearance to the craze-like structure (Fig. 6, inset). Deformation led to changes in kebab size, shape, and location, destroying the original lamellar character of this material.

Electron diffraction was used to determine the chain axis orientation within these highly deformed "crazed" regions. Reflections from fibrils within "crazed" regions were generally weak and broad but highly oriented along the fibril axis (Fig. 6, inset). The large peak breadth along the equator, and absence of essentially all reflections except the merged (1 1 0) and (2 0 0) reflections indicated that the samples had undergone significant decrystallization. The weakness of reflections was due to the small number of crystals in a given projected volume, a result of film thinning, cavitation, and extensive decrystallization within the highly deformed region.

3.4. Mechanical behaviour

The preceeding morphological observations were related to the known mechanical behaviour of HDPE at room temperature. The studies done here apply to highly oriented HDPE. During yielding, lamellae plastically deformed and fed into fibrils while non-crystalline regions extended. Further straining typically results in a significant increase in stress level (strain hardening) as a large portion of the chains become extended and stresses are taken up by covalent bonds along the extended chain backbone. Subsequent elongation occurred at the expense of the crystalline phase, which underwent decrystallization and brought about a further increase in chain extension. Darkfield microscopy (of samples viewed directly following deformation as well as several hours after deformation) did not reveal any noticeable deformation-induced crystallization. Apparently, the mobility and extension of chains at 25° C was not high enough to bring about strain-induced crystallization. It, therefore, appears that strain hardening in PE can occur even if there is an apparent loss of crystallinity, provided that chain extension increases with draw. However, as these materials were not drawn to failure, it is not yet clear whether strain-induced crystallization would occur at still higher strains than those accessed. Under appropriate conditions, HDPE is of course capable of strain-induced crystallization, as indicated for example by the presence of chain-extended shish crystals in the initial thin films. Moreover, strain-induced crystallization was observed for deformation at higher temperatures, as will be made evident in Part II of this series [25].

4. Conclusions

Thin, oriented, single-crystal-like textured, shish-kebab morphology films of HDPE were uniaxially extended both parallel and perpendicular to the chain direction. At low strains, the films formed cavitated regions spanned by fibrils. The presence of shish-kebabs was shown to influence cavity growth such that cavities nucleated and grew between shish-kebabs,

propagation perpendicular to the shish axis being hindered. This was attributed to the high yield stress of the crystalline phase at this temperature. The craze-like morphology resembled that outlined by Friedrich [29], except that tie fibrils interconnected "craze" fibrils in the present case. A decrystallization process enabled kebabs to feed into shish crystals, resulting in shish-kebab elongation. The shish-kebabs were transformed into fibrils which subsequently underwent draw-down.

Near isothermal deformation resulted in the mechanical transformation ("decrystallization") of crystals by $\langle 0\,0\,1 \rangle$ crystal shear, chain unfolding and slip, and the generation of "defects" within crystals. Crystal shear brought about a distortion in crystal block shape followed by a decrease in crystal width (perpendicular to the chain axis). More importantly, it was shown that a reduction in crystal thickness (parallel to the chain axis) could be brought about mechanically (by means of "defect" generation), without requiring a rise in temperature. The incorporation of defects within the lattice would in turn facilitate yielding. Both chain unfolding and defect generation would presumably lead to a loss of crystallinity as well. In addition, the crystalline phase underwent a martensitic transformation from the orthorhombic to monoclinic phase. Although non-crystalline phase elongation occurred, no newly formed crystalline regions indicative of strain-induced crystallization at room temperature were detected in darkfield micrographs.

The absence of observable strain-induced crystallization suggested that polyethylene comprised of two discontinuous phases prior to deformation will not develop a continuous crystalline phase upon isothermal deformation at room temperature. The strain hardening found in HDPE is apparently a result of non-crystalline phase extension, and an increase in the number of load-bearing bonds. In the bulk and at high strain rates, it is probable that deformation is non-isothermal. In that case, strain-induced crystallization would probably accompany deformation. These thin film studies are, however, applicable to studies of bulk PE because they show that changes in crystal thickness cannot be used as proof of thermally induced melting during deformation. In addition, they suggest that a loss of crystallinity can occur at temperatures below the standard melting range when a material is subject to stress. This is particularly relevant to bulk material deformed at low temperatures and low strain rates.

Acknowledgements

We thank the Materials Research Laboratory, University of Massachusetts for use of their facilities. This research was funded by the National Science Foundation, Grant #DMR84-06079 (Polymers Program).

References

1. R. J. SAMUELS, *Polym. Eng. Sci.* **25** (1985) 864.
2. R. A. DUCKETT, *Int. Met. Rev.* **28** (1983) 158.
3. A. PETERLIN, *Polym. Eng. Sci.* **19** (1979) 118.
4. G. CAPACCIO, T. A. CROMPTON, and I. M. WARD, *J. Polym. Sci. Phys. Edn* **14** (1976) 1641.
5. P. B. BOWDEN and R. J. YOUNG, *J. Mater. Sci.* **9** (1974) 2034.
6. I. M. WARD, *Polym. Eng. Sci.* **24** (1984) 724.
7. J. M. SCHULTZ, *ibid.* **24** (1984) 770.
8. P. SMITH, P. J. LEMSTRA, J. P. L. PIJPERS, and A. M. KIEL, *Colloid Polym. Sci.* **259** (1981) 1070.
9. M. TAKAYANAGI, K. IMADA, and T. KAJIYAMA, *J. Polym. Sci. Polym. Symp.* **15** (1966) 263.
10. J. C. HALPIN and J. L. KARDOS, *J. Appl. Phys.* **43** (1972) 2235.
11. A. G. GIBSON, G. R. DAVIES, and I. M. WARD, *Polymer* **19** (1978) 683.
12. A. PETERLIN, *J. Mater. Sci.* **6** (1971) 490.
13. T. SETO, T. HARA, and K. TANAKA, *Jpn. J. Appl. Phys.* **7** (1968) 31.
14. M. BEVIS and E. B. CRELLIN, *Polymer* **12** (1971) 666.
15. G. MEINEL and A. PETERLIN, *J. Polym. Sci. Part A2* **9** (1971) 67.
16. H. H. KAUSCH and K. L. DEVRIES, *Int. J. Fracture* **11** (1975) 727.
17. D. C. PREVORSEK, P. J. HARGET, R. K. SHARMA, and J. REIMSCHEUSSEL, *J. Macromolecular Sci. Phys.* **B8** (1973) 127.
18. A. PETERLIN, *J. Appl. Phys.* **48** (1977) 4099.
19. *Idem, Polym. Eng. Sci.* **18** (1978) 488.
20. F. DECANDIA, V. VITTORIA, and A. PETERLIN, *J. Polym. Sci. Phys.* **23** (1985) 1217.
21. M. MILES, J. PETERMANN, and H. GLEITER, *J. Macromolecular Sci.* **B12** (1976) 523.
22. R. CORNELUISSEN and A. PETERLIN, *Makromolekulare Chemie* **105** (1967) 193.
23. A.PETERLIN and K. SAKAOKU, *J. Appl. Phys.* **38** (1967) 4152.
24. A. PETERLIN, "Advances in Polymer Science and Engineering" edited by K. D. Pae, D. R. Morrow and Y. Chen (Plenum, New York, 1972) p. 1.
25. J. M. BRADY and E. L. THOMAS, *J. Mater. Sci.* to be published.
26. *Idem., Polymer.* to be published.
27. J. PETERMANN and R. M. GOHIL, *J. Mater. Sci.* **14** (1979) 2260.
28. J. M. BRADY and E. L. THOMAS, *J. Polym. Sci. Phys.* **26** (1988) 2385.
29. K. FRIEDRICH, "Advances in Polymer Science, 52/53" edited by H. H. Kausch (Springer Verlag, New York, 1983) p. 225.
30. A. R. POSTEMA, W. HOOGSTEEN, and A. J. PENNINGS, *Polym. Commun.* **28** (1987) 148.
31. B. HEISE, H. G. KILIAN, and W. WULFF, *Prog. Colloid Polym. Sci.* **67** (1980) 143.
32. H. MATSUDA, R. KASHIWAGI, M. OKABE, *Polymer J.* **20** (1988) 189.
33. T. SETO, T. HARA, and K. TANAKA, *Jpn J. Appl. Phys.* **7** (1968) 31.
34. W. W. ADAMS, D. YANG, and E. L. THOMAS, *J. Mater. Sci.* **21** (1986) 2239.
35. E. M. RECK, H. SCHENK and W. WILKE, *Prog. Colloid Polym. Sci.* **71** (1985) 154.
36. J. PETERMANN and H.GLEITER, *J. Mater. Sci.* **8** (1973) 673.
37. G. M. SWALLOWE, J. E. FIELD, and L. A. HORN, *ibid.* **21** (1986) 4089.
38. P. J. PHILLIPS and R. J. PHILPOT, *Polym. Commun.* **27** (1986) 307.
39. P. R. SWAN, *J. Polym. Sci.* **56** (1962) 403.
40. D. KRUEGER and G. S. Y. YEH, *J. Macromolecular Sci.* **B6** (1972) 431.
41. P. F. VAN HUTTEN, C. E. KONING, and A. J. PENNINGS, *Colloid Polym. Sci.* **262** (1984) 521 and references therein.
42. B. D. LAUTERWASSER and E. J. KRAMER, *Phil. Mag.* **A39** (1979) 469.

Received 6 July
and accepted 18 November 1988